INSTITUTE OF PHYSICS PUBLISHING NANOTECHNOLOGY
Nanotechnology **16** (2005) 555–566 doi:10.1088/0957-4484/16/4/037

Effect of randomly occurring Stone–Wales defects on mechanical properties of carbon nanotubes using atomistic simulation

Qiang Lu and Baidurya Bhattacharya[1]

Department of Civil and Environmental Engineering, University of Delaware, Newark, DE 19716, USA

E-mail: bhattacharya@ce.udel.edu

Received 13 October 2004, in final form 26 January 2005
Published 25 February 2005
Online at stacks.iop.org/Nano/16/555

Abstract
The remarkable mechanical properties of carbon nanotubes (CNTs) have generated a lot of interest in recent years. While CNTs are found to have ultra-high stiffness and strength, an enormous scatter is also observed in available laboratory results. This randomness is partly due to the presence of nanoscale defects, heterogeneities etc, and this paper studies the effects of randomly distributed Stone–Wales (SW or 5–7–7–5) defects on the mechanical properties of single-walled nanotubes (SWNTs) using the technique of atomistic simulation (AS). A Matern hard-core random field applied on a finite cylindrical surface is used to describe the spatial distribution of the Stone–Wales defects. We simulate a set of displacement controlled tensile loadings up to fracture of SWNTs with (6, 6) armchair and (10, 0) zigzag configurations and aspect ratio around six. A modified Morse potential is adopted to model the interatomic forces. We find that fracture invariably initiates from a defect if one is present; for a defect-free tube the crack initiates at quite random locations. The force–displacement curve typically behaves almost linearly up to about half way, although there is no obvious yield point. Three mechanical properties—stiffness, ultimate strength and ultimate strain—are calculated from the simulated force and displacement time histories. The randomness in mechanical behaviour resulting only from initial velocity distribution was found to be insignificant at room temperature. The mean values of stiffness, ultimate strength and ultimate strain of the tube decrease as the average number of defects increases, although the coefficients of variation do not show such a monotonic trend. The introduction of an additional defect has the most pronounced effect on the randomness in mechanical properties when the tube is originally defect free. We also find that, for a given mean number of defects in the tube, the zigzag configuration has less strength and less ultimate strain on average, but more uncertainty in its stiffness and ultimate strain, compared with the armchair tube.

(Some figures in this article are in colour only in the electronic version)

[1] Author to whom any correspondence should be addressed.

1. Introduction

1.1. Randomness in the mechanical properties of CNTs

The report by Iijima [1] of the existence of helical carbon microtubules triggered widespread interest in this special structure of carbon, now called carbon nanotubes (CNTs). Later, Ebbesen and Ajayan [2] reported the bulk synthesis of CNTs using a variant of the standard arc-discharge technique for fullerene synthesis under a helium atmosphere. Hamada *et al* [3] and Saito *et al* [4, 5] calculated the electronic properties of individual nanotubes. The Young modulus was measured by Treacy *et al* [6], Wong *et al* [7] and Falvo *et al* [8]. An interesting statistic by Terrones [9] has shown an exponential growth of the number of publications on CNTs: from fewer than 50 in 1993 to more than 1500 in 2001. The study of the carbon nanotube (CNT) has been motivated largely due to its extraordinary electronic and mechanical properties. The CNT is found to be among the most robust materials: it has high elastic modulus (order of 1 TPa), high strength (up to 150 GPa), good ductility (up to 15% max strain), flexibility to bending and buckling and robustness under high pressure [10–13]. The combination of these properties makes the carbon nanotube a potentially very useful material and CNTs are now used as fibres in composites, scanning probe tips, field emission sources, electronic actuators, sensors, Li ion and hydrogen storage and other electronic devices. Also, CNTs can be coated or doped to alter their properties for further applications [9].

A survey of recent studies on the elastic modulus and strength of single-walled and multi-walled carbon nanotubes (SWNTs and MWNTs) is listed in tables 1 and 2. The collected data clearly show a few features:

(i) the Young modulus of SWNTs is found to range from 0.31 to 1.25 Tpa and the Young modulus of MWNTs ranges from 0.1 to 1.6 TPa;
(ii) the Young modulus may depend on chiralities;
(iii) experiments roughly show a trend that Young's modulus drops quickly as the diameter of tubes increases;
(iv) the strength varies a lot from about 5 to 150 GPa;
(v) last but not least, these mechanical properties (elastic modulus, strength and failure strain) reported from experiments and analysis show *significant variation*.

Such variation has also been noticed by a few recent studies [14, 15]. As detailed in the next section, some of the factors that give rise to randomness in *mechanical* properties affect CNT *electronic* properties as well. An analytical understanding of these variations, their sources and how they can be controlled is essential before CNTs and CNT-based products can be considered for widespread use across industries.

The huge scatter in these properties is possibly due to the variation in tube sizes (diameter and length), chiralities, random defect distribution, local fluctuations in energies, variations in the chemical environment, errors in measurements and even different ways of defining the cross-sectional area. Effects of sizes and chiralities of nanotubes on their mechanical properties have been studied [7, 16, 17]; however, their roles are still not very clear. Tables 1 and 2 also show that the elastic modulus measured from tubes with similar diameters varies quite significantly. Although experimental measurement techniques vary in sophistication, it is still doubtful that measurement errors are fully responsible for the huge variation. The lack of consensus in defining the cross-sectional area [18, 19] can be rectified with a simple multiplicative factor and is not likely to be a major source of the randomness. Therefore, a substantial part of the random effect is believed to occur from random defects and/or local energy fluctuations. In this study, we focus on the role of randomly occurring defects, particularly Stone–Wales defects, in the mechanical properties and fracture of CNTs.

1.2. Effects of defects on the mechanical properties of CNTs

Defects such as vacancies, metastable atoms, pentagons, heptagons, Stone–Wales (SW or 5–7–7–5) defects, heterogeneous atoms, discontinuities of walls, distortion in the packing configuration of CNT bundles etc are widely observed in CNTs [40–44]. Such defects can be the result of the manufacturing process itself: according to an STM observation of the SWNTs' structure, about 10% of the samples were found to exhibit stable defect features under extended scanning [45]. Defects can also be introduced by mechanical loading [46, 47] and electron irradiation [40]. It is reasonable to believe that these defects are randomly distributed in CNTs.

Studies have shown that defects have significant influence on the formation as well as on the electronic and mechanical properties of CNTs [11, 43, 46]. It has also been suggested that oxygen sensitivity may be an effective metric of defect concentration in carbon nanotubes [48]. Pentagon and heptagon defects are believed to play key roles in the formation and deformation of CNTs. For example, with the help of pentagon and heptagons, one can build special structures based on the original hexagon lattice, such as capping, intramolecular junctions, variation in diameter or chirality, welding, coalescence, x-junction etc [43].

The Stone–Wales (SW) defect, which is the focus of this paper, is composed of two pentagon–heptagon pairs, and can be formed by rotating a sp^2 bond by 90° (SW rotation). SW defects are stable and commonly present in carbon nanotubes [49], and are believed to play important roles in the mechanical [15, 50], electronic [51], chemical [52], and other properties of carbon nanotubes. For example, Chandra *et al* [15] found that the SW defect significantly reduced the elastic modulus of single-walled nanotubes. Mielke *et al* [53] compared the role of various defects (vacancies, holes and SW defects) in fracture of carbon nanotubes, and found that various one- and two-atom vacancies can reduce the failure stresses by 14 to 26%. The SW defects were also found to reduce the strength and failure strain, although their influence was less significant than vacancies and holes.

It has been found that SWNTs, under certain conditions, respond to the mechanical stimuli via the spontaneous formation of SW defects beyond a certain value of applied strain around 5%–6% [47]. Atomistic simulations showed that these SW defects are formed when bond rotation in a graphitic network transforms four hexagons into two pentagons and two heptagons, which is accompanied by elongation of the tube structure along the axis connecting the pentagons, and shrinking along the perpendicular direction. More interestingly, the SW defect can introduce successive SW

Table 1. A survey of mechanical properties of SWNTs.

Ultimate strength (GPa)	Young's modulus (TPa)	Diameter (nm)	Length (nm)	Source, method/Comment
NA	1.25–0.35/ +0.45	1.0–1.5	23.4–36.8	[20] Thermal vibration experiment.
NA	0.97–1.20	0.4–3.4	10	[21] AS using EAM potential. Modulus increases significantly with decreasing diameter and increases slightly with decreasing helicity.
NA	0.8–1.22	0.8–2.0	NA	[18] *Ab initio* calculation. Modulus depends on chiralities.
NA	0.50–0.82	0.6–1.4	Infinite[a]	[19] *Ab initio* calculation. Very little dependence on diameters and chiralities.
$\geqslant 45 \pm 7$	NA	1.1–1.4	>4000	[22] AFM bending test on SWNT ropes. Maximum strain is measured as $(5.8 \pm 0.9)\%$, strength is calculated by assuming E is 1.25 TPa.
NA	0.97	0.68–27	NA	[23] Empirical force constant model.
NA	0.4–0.8	2.4–3.3	NA	[24] AS using Brenner's potential, tensile loading.
NA	0.50	0.4–2.2	Infinite[a]	[25] AS using Brenner's potential, tensile loading.
NA	0.98	1.3	14	[26] Tight binding.
NA	1.2	3.1 ± 0.2	NA	[27] 3-point bending.
NA	5.0	0.68	NA	[28] Tight-binding calculation, wall thickness 0.7 Å.
NA	4.70	NA	NA	[29] Local density approximation model, wall thickness 0.75 Å.
65–93	NA	1.6	NA	[30] AS using modified Morse model, tensile loading.
62.9	0.83–3.02	0.68	NA	[31] Atomistic simulation and *ab initio* calculation, w/o defects.
40–50	1.0	0.4–2.2	6–1000	[32] Theoretical analysis based on AS. Modulus, yield strain and strength. depend on loading rate. Yield strain depends on tube length.
4.92	0.311	1.36	NA	[33] Tight-binding simulation, maximum strain 22%. Poisson ratio 0.287. Modulus slightly depends on diameters.

[a] Simulating infinite long tube with periodic boundary condition.

Table 2. A survey of mechanical properties of MWNTs.

Ultimate strength (GPa)	Young's modulus (TPa)	Outer diameter (nm)	Length of tube (nm)	Method/comment
14.2 ± 8.0	1.28 ± 0.59	26–76	8.0	[7] Buckling stress is measured, which should be smaller than tensile strength. No dependence of Young's modulus on tube diameter.
100–150	NA	21	Buckling: 18.3–68 Bending: 800	[8] Both bending and buckling tests are conducted. The strength is calculated from a maximum strain of 16% from bending.
55	NA	8.4–16.6	46.2–436	[34] Critical buckling stress is measured.
135–147	NA	19.6–56.2	Buckling length: 47–223.5	[35] Critical buckling stress is measured.
11–63	0.27–0.95	13–33	6900–11 000	[36] Strength measured through direct stretching. Failure occurs when the outermost layer is broken. No apparent dependence of tensile strength on the outer shell diameter. 12% strain at failure is measured.
150	$0.91 \pm 20\%$	<10	About 500	[37] Strength measured through direct stretching.
NA	0.6–1.1	10–20	NA	[6] Elastic modulus is measured through thermo-vibration method; higher modulus is found for thinner tubes.
NA	0.1–1.6	12–30	1500–6250	[16] Elastic modulus is measured through resonant vibration, and found to decrease sharply with increasing diameter.
NA	<0.12	30–250	About 2000	[38] Elastic modulus is measured through resonant vibration, and found to increase rapidly as diameter decreases.
NA	0.67–1.1	$4.8–16.0 \pm 5\%$	240–420	[39] Elastic modulus is measured through beam deflection, and no significant dependence found on diameter.

rotations of different C–C bonds, which lead to a gradual increase of tube length and shrinkage of tube diameter, resembling the necking phenomenon in tensile tests at the macro-scale. This process also gradually changes the chirality of the CNT, from the armchair to the zigzag direction. This whole response is plastic, with necking and growth of a 'line defect', resembling the dislocation nucleation and moving in plastic deformation of the crystal in many ways. Yakobson [54] thus applied the dislocation theory and compared the brittle and ductile failure paths after the nucleation of the SW defect.

The formation of SW defects due to mechanical strains has also been reported by other groups of researchers. In their atomistic simulation study, Liew *et al* [50] showed that SW defects were formed at 20–25% tensile strain for single-walled and multi-walled nanotubes with chirality ranging from (5, 5) to (20, 20). The formation of SW defects explained the plastic behaviour of the stress–strain curve. They also predicted failure strains of these tubes to be about 25.6%. A hybrid continuum/atomistic study by Jiang *et al* [55] reported the nucleation of SW defects both under tension and torsion.

The reported SW transformation critical tensile strain is 4.95%, and critical shear strain is 12%. The activation energy and formation energy of the SW defect formation are also studied and related to the strength of the nanotube [56–58]. The nucleation of SW defects was found to depend on the tube chiralities, diameters and external conditions such as temperature.

It is important to mention here that the above studies [47, 50, 54, 55] are all based on the bond order potential model. Two recent studies critical of the bond order model must also be mentioned in this context. Dumitrica *et al* [59] argued that the energy barrier for SW defect formation at room temperature is high enough to inhibit stress-induced SW defect formation, and showed that direct bond breaking is a more likely failure mechanism for defect-free nanotubes. A quantum mechanical study [60] from the same group pointed out that the results in [47] and related works were not reliable since the potential model they used (i.e., the bond order model) was not capable of correctly describing breaking of the bond connecting the two pentagons in the SW pair. They [60] further found that pre-existing SW defects caused successive bond breakings instead of bond rotations as reported by [47, 50, 54, 55]. Nevertheless, irrespective of how SW defects are formed and grow, it is clear that they can have significant effects on the mechanical properties of carbon nanotubes.

In conclusion, it is clear that

(i) defects are commonly present in CNTs,
(ii) these defects may have significant effects on the mechanical and other properties of CNTs, as summarized in tables 1 and 2,
(iii) a wide scatter has been observed in the mechanical properties of carbon nanotubes.

Yet, surprisingly little work has been directed in the available literature toward studying the randomness in these defects and the influence of such randomness on CNT mechanical properties in a systematic and probabilistic way. Here in this paper, we try to build toward this missing link by selecting the effect of randomly occurring Stone–Wales defects in SWNTs as a potentially significant case study. We make reasonable assumptions on the random nature of the SW defects and, through the technique of atomistic simulation, quantify the effect of such randomness on (i) the fracture process of SWNTs at the atomic scale and (ii) three representative mechanical properties, namely, the elastic modulus, ultimate strength and ultimate strain of SWNTs.

2. Modelling of random Stone–Wales defects

An ideal modelling of material defects would require a real 3D random field model. However, since each SW defect on an SWNT is a local rearrangement of carbon atoms on the tube wall, we can treat the SW defects as discs with a fixed area that are randomly distributed on the 2D surface. This way, it is sufficient to consider two characteristics of the defect distribution: (i) the location of the points relative to the study area, and (ii) the location of points relative to each other.

To our knowledge, there are few published works to date that study the effects of random defects, especially of the Stone–Wales kind, on the mechanical properties of CNTs. The study by Saether [44] investigated the transverse mechanical properties of CNT bundles subject to random distortions in their packing configuration. This distortion, quantified by a vector describing the transverse displacement of the CNTs, may be caused by packing faults or inclusions. The magnitude and direction of the vector were both uniform random variables. The transverse moduli of CNT bundles were found to be highly sensitive to small distortions in the packing configuration. In another instance, Belavin *et al* [61] studied the effect of random atomic vacancies on the electronic properties of CNTs. Each of the N_a atoms in the 'unit cell' was assigned (using an unspecified numbering scheme) a unique id in the range $[1, N_a]$. A first estimate of the number of atoms to be removed was made by generating a uniform deviate, n_d, in the interval $[1, N_a]$. It is not apparent how the n_d atoms to be removed were identified. However, the atoms in this set were removed from the unit cell provided the cell was left with atoms with coordination numbers of two or three. That is, (i) the removal of an atom did not give rise to an additional dangling bond, or, (ii) if it did, the additional removal of the candidate's neighbour rectified the situation. Belavin *et al*'s model is simple and effective for generating vacancies, but its physical basis as a 2D spatial random field model is not clear and it cannot be extended to areal defects involving more than one atom such as a SW defect.

Since there is not enough information in the experimental literature to provide a clear picture of statistical properties of the defects, it is reasonable to start with the assumption that the defects occur in a completely random manner, which implies an underlying homogeneous Poisson spatial process. We also incorporate the fact that the SW defect is not a point defect but has a finite area and there should be no overlap between neighbouring defects. Therefore, we adopt a Matern hard-core point process [62] for the defect field. A Matern hard-core process is simply a thinned Poisson point process in which the constituent points are forbidden to lie closer than a minimum distance h.

The intensity (i.e., rate of occurrence) of the Matern hard-core process is $\lambda_h = p_h\lambda$ where λ is the intensity of the underlying homogeneous Poisson point process and p_h is the probability that an arbitrary point from the underlying Poisson process will survive the Matern thinning. The average number of SW defects on an area A_t is thus $\lambda_h A_t$. For a finite tube of length b, the probability p_h can be computed as

$$p_h = \frac{1}{b}\int_0^b \frac{1 - e^{-\lambda A(y)}}{\lambda C(y;h)}\,dy \qquad (1)$$

where C is the area over which a Poisson point at (x_0, y_0) searches for its neighbours [63].

In this study, we fix h at 8.0 Å, and use a set of reasonable values for λ. The algorithm for generating SW defects is outlined in figure 1. An application of the algorithm is illustrated on a graphene sheet in the following. In this particular example, the graphene sheet is 49.2 Å long and 25.5 Å wide and is used to create a (6, 6) armchair SWNT. The SWNT ends up with six SW defects.

Random points are generated uniformly on the graphene sheet with rate λ per unit area (to conform to a Poisson spatial process) and the points are assigned integer ids in the order

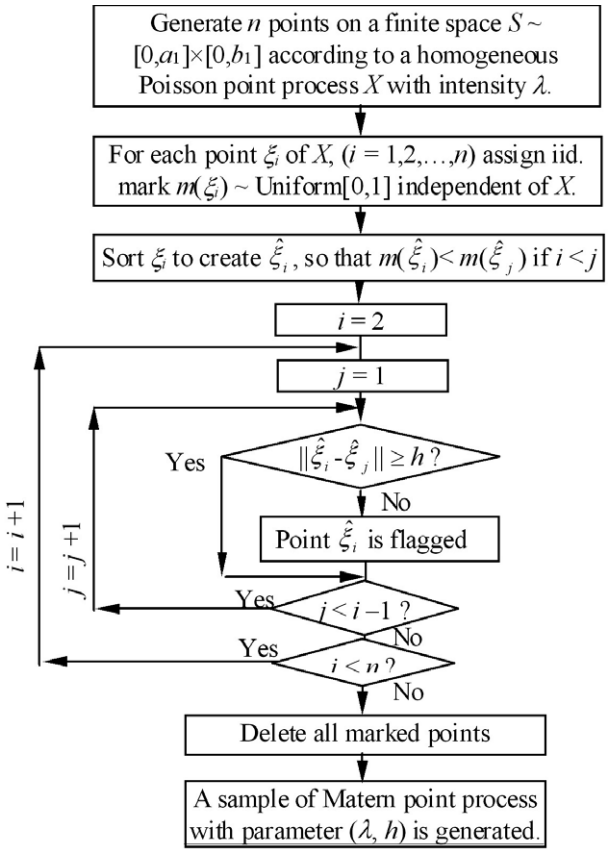

Figure 1. Generating a Matern hard-core field.

they are generated (figure 2(a)). Eight Poisson points are generated in this example. The distance between every pair of points is checked. If a pair of points is less than h apart, the point with the smaller id in that pair is marked (figure 2(b)). Once all pairs are compared, the marked points are deleted, thus producing a Matern hard-core field. In this example, two points (numbers 4 and 5) are deleted to produce the hard-core field. For each surviving point, the closest carbon–carbon bond on the graphene sheet is located (figure 2(c)) and the bond is rotated by 90° to form an SW defect (figure 2(d)). The graphene sheet with the six SW defects is shown in figure 3(a); the corresponding armchair SWNT is shown in figure 3(b).

3. Mechanical behaviour of SWNTs with random SW defects

Due to the small size of carbon nanotubes, laboratory experiments to measure their mechanical properties are difficult and potentially expensive at the current state of the art. Atomistic simulation or AS, therefore, is a very attractive tool that can complement laboratory experiments in studying the mechanical behaviour and failure of small-scale structures such as carbon nanotubes, particularly when heterogeneities and the discrete nature of the material becomes dominant [64]. Although AS has a natural advantage over classical continuum based approaches in studying small-scale mechanics, we should also mention that elegant continuum approaches have been used to study the mechanical properties of carbon nanotubes [17, 65–70]. These continuum approaches are computationally efficient compared with atomistic simulation; however, they both have limitations. They apply well to the *defect-free* nanostructure; the quasi-continuum approach is especially preferred when the deformation is uniform, so that a closed form strain energy can be derived and the mechanical properties can be solved analytically. Moreover, they are both intrinsically static (the kinetic energy of the atoms is not considered), making it more difficult to study dynamic properties. Finally, to the knowledge of the authors, these continuum based methods have not been applied to study properties of nanotubes in the presence of randomness.

For the atomistic simulation part of this study, a modified Morse potential model for describing the interaction among carbon atoms [71] is applied. This potential model does not have some of the shortcomings of the bond order potential models; for example, the cut-off function in Brenner's bond order model is said to give rise to spurious forces and inaccurately large breaking strain [30, 60, 72].

The bond-breaking criterion is an important issue in the simulation of fracture of solids. Most atomistic simulation studies adopt a distance-based criterion (r_f) for this; i.e., the bond between atoms is regarded as broken if the separation between atoms exceeds a critical distance [73–77]. A good guess is that r_f is equivalent to the cut-off distances r_c of potential energy functions. Based on studies such as [31, 59], we adopt the cut-off distance (r_c) and the critical inter-atomic separation (r_f) as $r_f = r_c = 1.77$ Å in this example.

In order to study the effects of Stone–Wales defects on mechanical properties and the fracture process of carbon nanotubes, we adopt two single-walled nanotube (SWNT) configurations in this study: the (6, 6) armchair having diameter 8.14 Å and the (10, 0) zigzag having diameter 7.82 Å. The total number of atoms in the simulation was 460 for the 49.2 Å long (10, 0) zigzag tube and 480 for the 49.2 Å long (6, 6) armchair tube.

The initial atomic positions are obtained by wrapping a graphene sheet (a typical example is shown in figure 3) into a cylinder along the chiral vector $C_n = m\mathbf{a}_1 + n\mathbf{a}_2$ such that the origin (0,0) coincides with the point (m, n). The distance between neighbouring carbon atoms on the graphene sheet, a_0, is 1.42 Å, which is the C–C sp^2 bond length in equilibrium. The tube diameter is thus obtained as $d = a_0\sqrt{3(m^2 + n^2 + mn)}/\pi$.

The initial atomic velocities are randomly chosen according to a uniform distribution (between the limits -0.5 and 0.5) and then rescaled to match the initial temperature (300 K in this example). We assume that the nanotube is in vacuum or in air, and the heat conduction between the tube and the environment is relatively small compared to the heat accumulation from the mechanical loading at high speeds. From test runs, the temperature fluctuations in the simulations are found to be within acceptable ranges. Therefore, no temperature control is implemented in this study. The mechanical loading is uniaxial and displacement controlled: it is applied by moving the atoms at either end (12 atoms at each end, as shown in figure 4) in the axial direction away from each other at constant speed (10 m s^{-1}) without relaxing until the occurrence of fracture.

Three mechanical properties are calculated from the simulated force and displacement time histories:

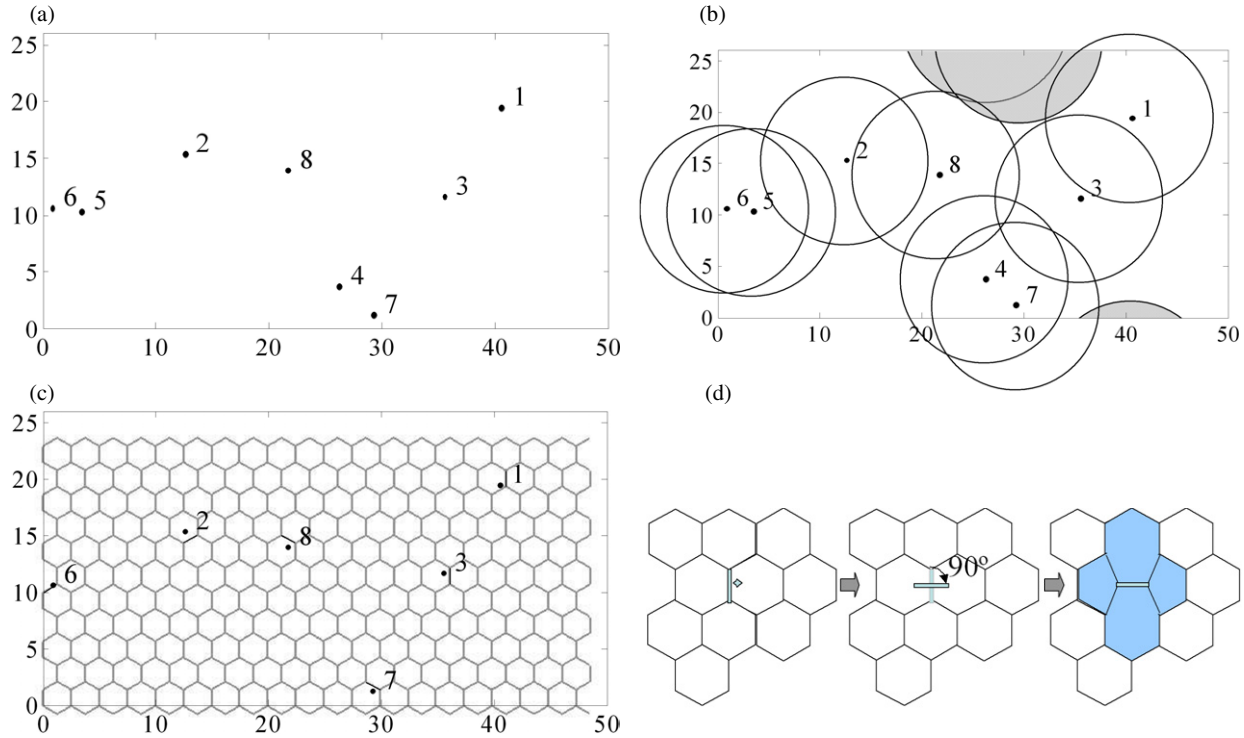

Figure 2. Generation of Stone–Wales defects on a graphene sheet. (a) Poisson points are generated on a plane. (b) Pairs of points less than h apart are identified. (c) The Matern hard-core field is produced by thinning the Poisson field. (d) SW defects are generated by rotating the C–C bond.

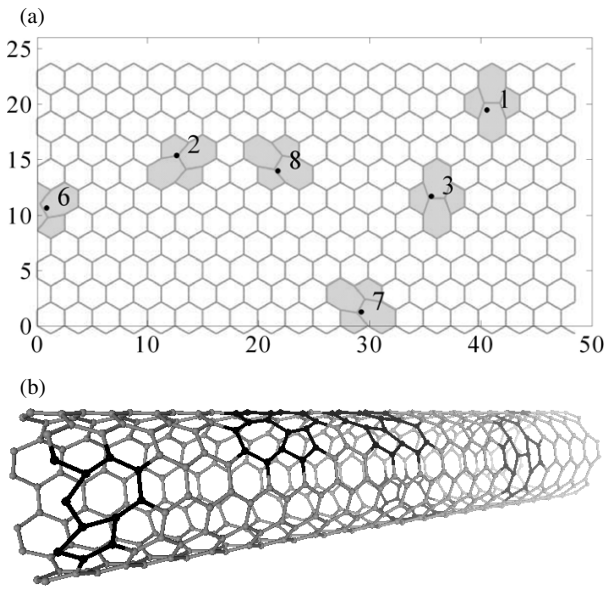

Figure 3. (a) Graphene sheet with six SW defects; (b) the corresponding (6, 6) SWNT.

(i) the Young modulus is calculated as the initial slope of the force–displacement curve;

(ii) the ultimate strength is calculated at the maximum force point, $\sigma_u = F_{max}/A$, where F is the maximum axial force, A is the cross section area, assuming the thickness of tube wall is 0.34 nm;

(iii) the ultimate strain, which corresponds to the ultimate strength, is calculated as $\varepsilon_u = \Delta L_u/L$, where L is the original tube length.

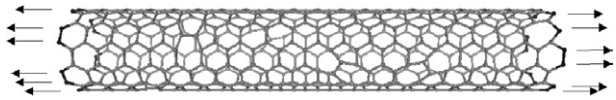

Figure 4. Mechanical loading is applied through moving the outermost atoms at both ends (highlighted at bond ends).

Other important information can also be obtained through the simulation of tensile tests of SWNTs, such as the time histories of energies and bond angles, dependence of mechanical properties on diameter, chirality and loading rate etc [17–19, 21, 32, 64].

Examples of the force–displacement relations of a (6, 6) SWNT are shown in figure 5, with the same initial velocity distribution in each case but with different numbers of SW defects (0, 2, 4, 6, respectively). The displacement controlled loading rate is 10 m s^{-1}. The reduced units (ru) used in this and subsequent figures have the following physical equivalents: 1 time ru = 0.035 26 ps; 1 force ru = 1.602 nN; 1 displacement ru = 1 Å.

It is clear from figure 5 that defects can have significant impact on mechanical behaviour of nanotubes: SWNTs with more defects are likely to break at smaller strains and have less strength as well. The force–displacement curve in each case in figure 5 behaves almost linearly up to about half way, although there is no obvious yield point. The slope then begins to decrease up to the breaking point where an abrupt drop of force occurs. The effect of defects on the Young modulus, however, appears much less pronounced.

Eight snapshots taken from the fracture process of a defect-free (6, 6) armchair SWNT are shown in figure 6(a), illustrating the detailed crack evolution from the first bond breaking to the

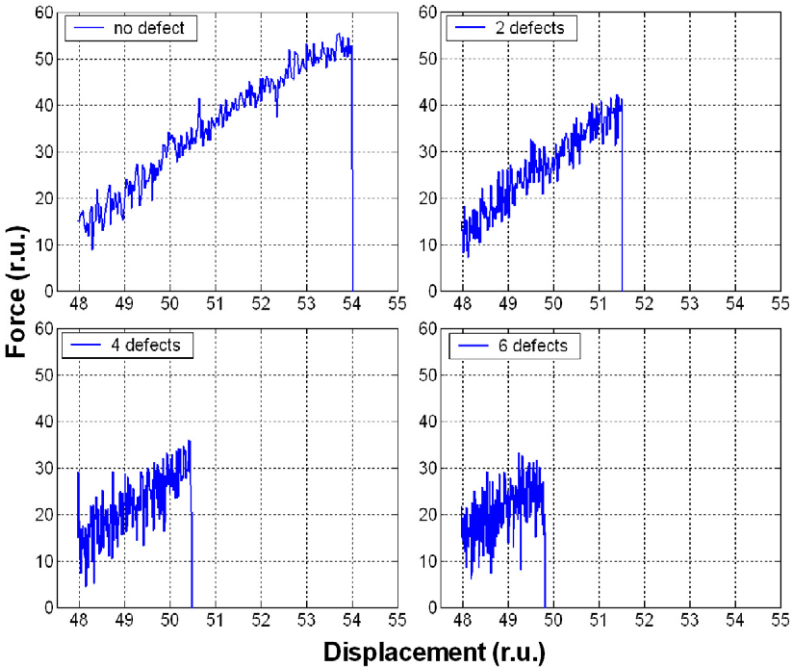

Figure 5. Force–displacement curves of nanotubes with various average numbers of defects.

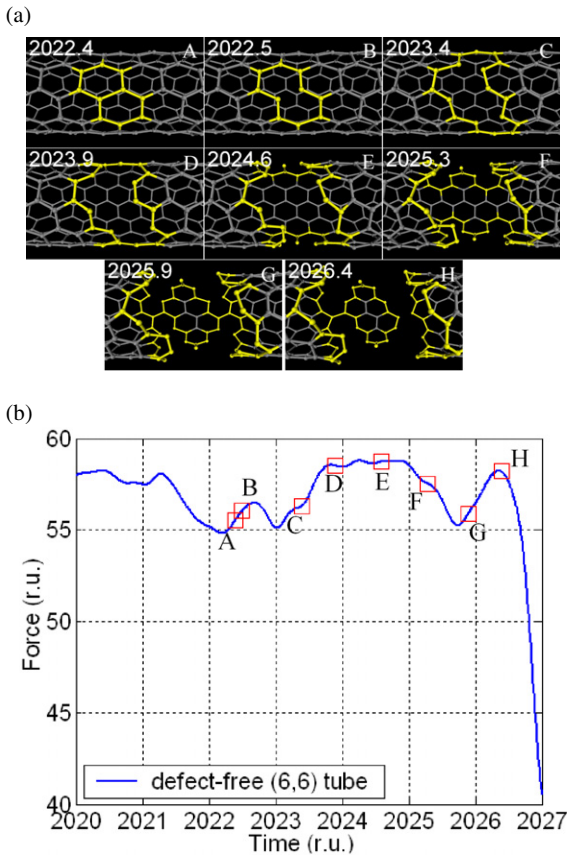

Figure 6. Fracture process of a defect-free (6, 6) SWNT: (a) crack initiation and propagation (A–H); (b) corresponding force time history.

complete separation into two parts. Figure 6(b) shows the corresponding time instants of these snapshots on the force time history. The fracture process of a similar (6, 6) armchair SWNT but with three Stone–Wales defects is studied next (figure 7(a)). The corresponding force time history is shown in figure 7(b), showing that the SWNT breaks much earlier than the defect-free tube under identical loading. The crack initiates from a heptagon, and grows irregularly until it breaks the tube. This is representative of all subsequent tensile simulations of SWNTs with defects: cracks invariantly initiate from a defect and grow irregularly. For a defect-free tube, in contrast, the crack initiates at quite random locations (as shown in figure 8) on the tube surface and grows at an angle of about 60° with the tube axis in the case of the (6, 6) armchair, and at about 90° with the tube axis in the case of the (10, 0) zigzag. The only source of randomness in figure 8 is in the initial velocity distribution of the atoms. The tube length in each case in figure 5 through figure 8 is constant at 49.2 Å as is the displacement controlled loading rate at 10 m s^{-1}.

The effects of randomness in the spatial distribution of SW defects on mechanical behaviour are now investigated for both the armchair and zigzag SWNTs. The tube length in each case is 49.2 Å while the displacement controlled loading rate is constant at 10 m s^{-1}. For each tube, we start with the defect-free case ($\lambda = 0$) and carry out 50 simulations leading to fracture. From these 50 samples we determine the statistics of the SWNT mechanical properties as shown in table 3. The only source of randomness here is in the distribution of the initial atomic velocities. The resultant coefficient of variation (c.o.v.) of Young's modulus (∼1% for armchair and ∼2% for zigzag) as well as that of ultimate strength (about 2% for either configuration) are negligible. The cov of ultimate strain, though higher at around 5%, is still rather small. Hence it is clear that, at the given temperature of 300 K, the randomness resulting from initial velocity distribution is insignificant.

We then move on to studying four cases with randomly occurring SW defects corresponding to four different mean field values, starting from an average of 0.9 defects per tube

Table 3. Young's modulus, ultimate strength and ultimate strain of SWNTs with different SW defect intensities.

Mean Poisson points λA_t	Mean Matern discs $\lambda_h A_t$	E^a (TPa)		$\sigma_u{}^a$ (GPa)		$\varepsilon_u{}^a$	
		μ	V (%)	μ	V (%)	μ (%)	V (%)
(6, 6) armchair							
0	0	0.851	1.01	105.5	2.01	12.45	4.93
1.0	0.925	0.793	5.50	89.71	13.80	8.69	33.91
2.0	1.716	0.771	6.25	83.11	13.52	7.20	36.05
4.0	2.970	0.738	7.77	76.29	10.02	5.50	29.56
6.0	3.889	0.716	6.76	74.56	8.93	4.94	31.61
(10, 0) zigzag							
0	0	0.831	2.17	86.78	1.85	8.88	4.89
1.0	0.925	0.778	7.15	74.53	12.52	5.71	39.85
2.0	1.716	0.775	7.89	70.17	14.75	4.75	49.56
4.0	2.970	0.750	10.17	65.80	7.12	3.57	30.25
6.0	3.889	0.711	14.78	63.05	9.12	2.89	43.59

[a] Based on statistics of 50 samples; μ = mean; V = coefficient of variation (c.o.v.), E = Young's modulus, σ_u = ultimate strength, ε_u = ultimate strain (strain at max force).

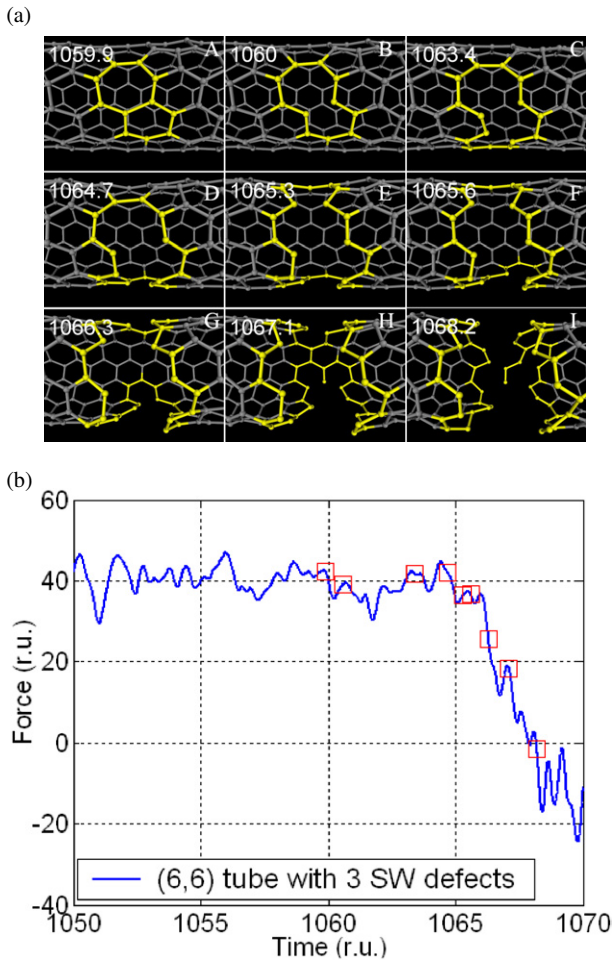

Figure 7. Fracture process of a (6, 6) SWNT with three SW defects: (a) crack initiation and propagation (A–I); (b) corresponding force time history.

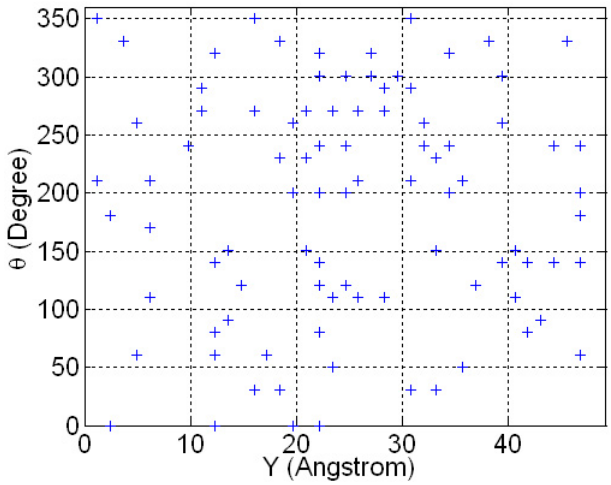

Figure 8. 2D spatial distribution of crack initiation site in defect-free (6, 6) SWNT (99 samples).

up to 3.9 mean defects per tube. For each mean value, 50 SWNT samples with defects are generated according to a Matern hardcore process, and loading leading to fracture is simulated as before. In order to systematically study the effects of spatial randomness, the initial velocity distributions are kept identical to those in the respective 50 defect-free cases. Figure 9 elaborates the effect of mean number of defects on the SWNT Young's modulus. It is clear that the scatter in the Young modulus increases with more defects and the tube becomes more compliant as well. The variation in the Young modulus in figure 9 agrees with experimental results reported in tables 1 and 2. Complete statistics of the mechanical properties of the tubes with defects are listed in table 3 and the trend is graphed in figure 10.

We clearly notice that the mean values of stiffness, strength and ultimate strain of the tube for either configuration decrease as the average number of defects increases. However, the uncertainty associated with each property (quantified by the c.o.v.) does not show such a monotonic trend in each case. Except for the Young modulus of the zigzag tube, it is rather interesting to note that the c.o.v.s of these properties reach their respective maxima when the average number of defects is in the range 1–3. Nevertheless, the most striking observation is perhaps that the introduction of an additional defect has the most pronounced effect on the randomness in mechanical properties when the tube is originally defect free than when one or more defects are already present.

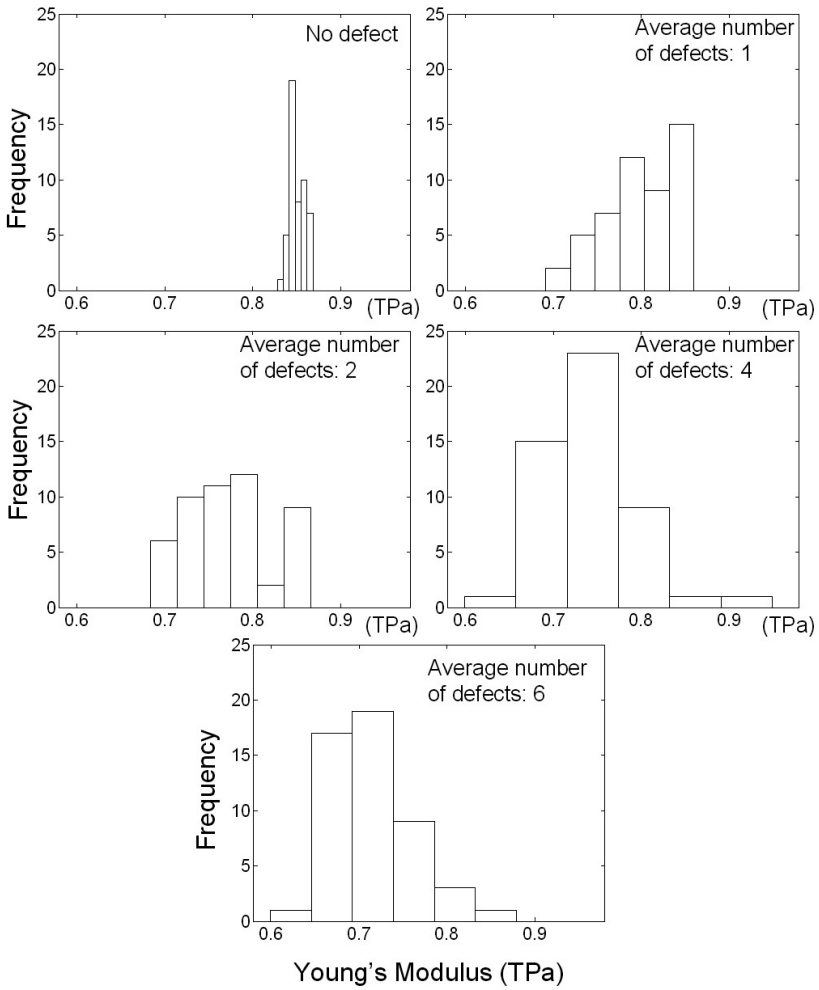

Figure 9. Distribution of Young's modulus of (6, 6) armchair nanotubes as a function of average number of SW defects (50 samples each).

The zigzag tube differs from the armchair one in two ways. For a given mean number of defects per tube, (i) the zigzag configuration has less strength and less ductility on average than the armchair tube although the mean stiffness is about the same; and (ii) the zigzag configuration shows more uncertainty in its stiffness and ultimate strain compared with the armchair tube although the strength has roughly the same c.o.v. in either configuration. The fact that the zigzag tube has less ultimate strain has been reported by a few studies [46, 56] and the widely observed fact that the brittle fracture mode is more sensitive to random defects has been corroborated by the above findings.

No dislocations similar to what was reported in other simulations [46, 47] were observed in our simulations. This may be due to the difference in the potential models and/or the loading modes: our tensile loading is continuous and monotonic at room temperature and we used a modified Morse potential, while Nardelli *et al* [47] used a bond order potential model and allowed unloading and relaxation at high temperature.

4. Summary and conclusions

Carbon nanotubes are known to have ultra-high stiffness and strength, yet a wide scatter has been observed in the mechanical properties of carbon nanotubes. It is likely that defects, which are commonly present in CNTs, may have significant effects on the mechanical and other properties of CNTs. In this paper we have considered the random nature of Stone–Wales (SW or 5–7–7–5) defects in CNTs and, through the technique of atomistic simulation, demonstrated that randomly occurring defects can have a significant influence on the fracture process and mechanical properties of SWNTs. A Matern hard-core random field applied on a finite cylindrical surface was used to describe the spatial distribution of the Stone–Wales defects.

We simulated a set of displacement controlled tensile loadings up to fracture of SWNTs with (6, 6) armchair and (10, 0) zigzag configurations. The force–displacement curve typically behaved almost linearly up to about half way, although there was no obvious yield point. The stiffness, strength and ultimate strain were calculated from the simulated force and displacement time histories. We found that fracture invariably initiated from a defect if one was present and the crack grew irregularly. For a defect-free tube, the only source of randomness was in the initial velocity distribution of the atoms, and the crack initiated at quite random locations on the tube surface.

The effects of randomness in the spatial distribution of SW defects on mechanical behaviour were investigated. Along with the defect free-case, we studied four cases with randomly

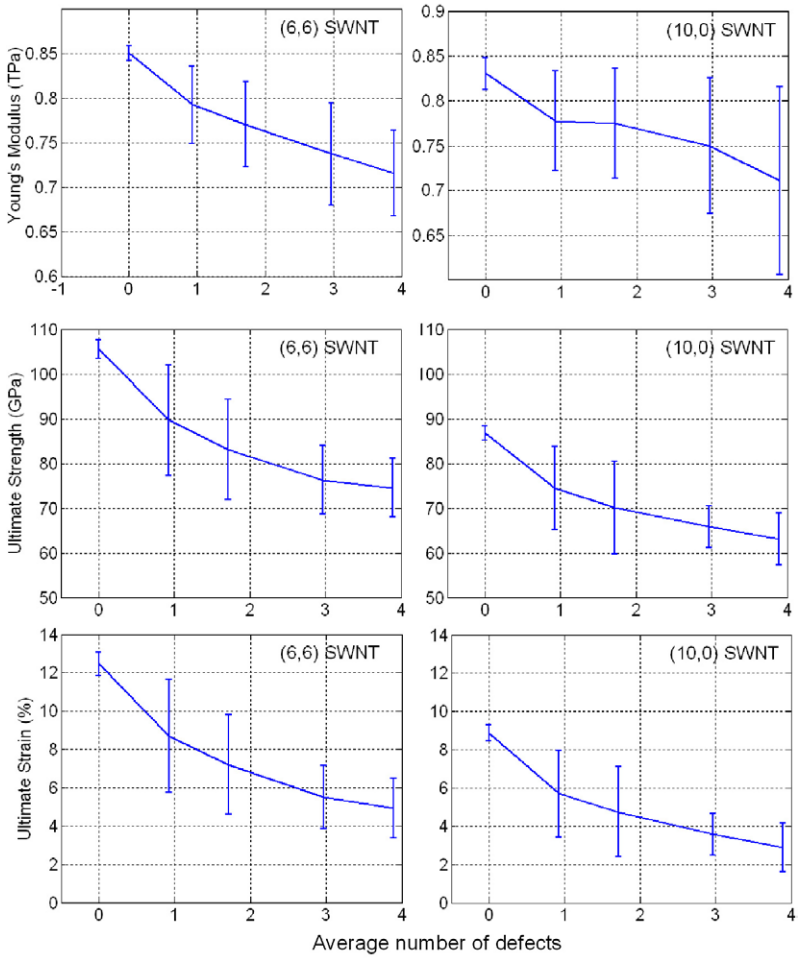

Figure 10. Effects of random SW defects on mechanical properties of armchair and zigzag SWNTs ($l = 49.2$ Å, 50 samples each). Solid line represents mean value, vertical bar implies +/− one standard deviation.

occurring SW defects starting from an average of 0.9 defects per tube up to 3.9 mean defects per tube. The randomness resulting solely from the initial velocity distribution (i.e., the defect free case) was rather insignificant at the operating temperature of 300 K. The mean values of stiffness, strength and ultimate strain of the tube decreased as the average number of defects increased. However, the uncertainty associated with each property did not show such a monotonic trend in each case. The introduction of an additional defect had the most pronounced effect when the tube was originally defect free than when one or more defects were already present. The zigzag tube was found to be more brittle and to exhibit more uncertainty in its mechanical properties than the armchair one.

Future work should be extended to more types of defects such as vacancies, heterogeneous atoms etc and more complicated structures. Experimental studies on the statistical distribution of such defects and of mechanical properties of nanotubes are also required for validation purposes.

Acknowledgment

A set of preliminary results from this work was presented at the 17th ASCE Engineering Mechanics Conference held at the University of Delaware, Newark, DE, USA, in June 2004.

References

[1] Iijima S 1991 Helical microtubules of graphitic carbon *Nature* **354** 56
[2] Ebbesen T W and Ajayan P M 1992 Large-scale synthesis of carbon nanotubes *Nature* **358** 220
[3] Hamada N, Sawada S and Oshiyama A 1992 New one-dimensional conductors: graphitic microtubules *Phys. Rev. Lett.* **68** 1579–82
[4] Saito R *et al* 1992 Electronic structure of graphene tubules based on C60 *Phys. Rev.* B **46** 1804–11
[5] Saito R *et al* 1992 Electronic structure of chiral graphene tubules *Appl. Phys. Lett.* **60** 2204
[6] Treacy M M *et al* 1996 Exceptional high Young's modulus observed for individual carbon nanotubes *Nature* **381** 678
[7] Wong E W, Sheehan P E and Lieber C M 1997 Nanobeam mechanics: elasticity, strength, and toughness of nanorods and nanotubes *Science* **277** 1971–5
[8] Falvo M R *et al* 1997 Bending and buckling of carbon nanotubes under large strain *Nature* **389** 582
[9] Terrones M 2003 Science and technology of the twenty-first century: synthesis, properties, and applications of carbon nantoubes *Annu. Rev. Mater. Res.* **33** 419–501
[10] Bernholc J, Brenner D and Nardelli M B 2002 Mechanical and electrical properties of nanotubes *Annu. Rev. Mater. Res.* **32** 347–75
[11] Yakobson B I and Avouris P 2001 Mechanical properties of carbon nanotubes *Top. Appl. Phys.* **80** 287–327

[12] Ruoff R S and Lorents D C 1995 Mechanical and thermal-properties of carbon nanotubes *Carbon* **33** 925–30
[13] Salvetat J P, Bonard J M and Thomson N H 1999 Mechanical properties of carbon nanotubes *Appl. Phys.* A **69** 255–60
[14] Sears A and Batra R C 2004 Macroscopic properties of carbon nanotubes from molecular-mechanics simulations *Phys. Rev.* B **69** 235406
[15] Chandra N, Namilae S and Shet C 2004 Local elastic properties of carbon nanotubes in the presence of Stone–Wales defects *Phys. Rev.* B **69** 094101
[16] Poncharal P *et al* 1999 Electrostatic deflections and electromechanical resonances of carbon nanotubes *Science* **283** 1513–6
[17] Li C Y and Chou T W 2003 Elastic moduli of multi-walled carbon nanotubes and the effect of van der Waals forces *Compos. Sci. Technol.* **63** 1517–24
[18] Hernandez E, Goze C and Bernier P 1998 Elastic properties of C and BxCyNz composite nanotubes *Phys. Rev. Lett.* **80** 4502–5
[19] Sanchez-Portal D *et al* 1999 *Ab initio* structural, elastic, and vibrational properties of carbon nanotubes *Phys. Rev.* B **59** 12678–88
[20] Krishnan A *et al* 1998 Young's modulus of single-walled nanotubes *Phys. Rev.* B **58** 14013–9
[21] Yao N and Lordi V 1998 Young's modulus of single-walled carbon nanotubes *J. Appl. Phys.* **84** 1939
[22] Walters D A *et al* 1999 Elastic strain of freely suspended single-wall carbon nanotube ropes *J. Appl. Phys.* **74** 3803–5
[23] Lu H, Rafii-Tabar H and Cross M 1997 Molecular dynamics simulation of fractures using an N-body potential *Phil. Mag. Lett.* **75** 237–44
[24] Cornwell C F and Wille L T 1998 Simulations of the elastic response of single-walled carbon nanotubes *Comput. Mater. Sci.* **10** 42–5
[25] Halicioglu T 1998 Stress calculations for carbon nanotubes *Thin Solid Films* **312** 11–4
[26] Ozaki T, Iwasa Y and Mitani T 2000 Stiffness of single-walled carbon nanotubes under large strain *Phys. Rev. Lett.* **84** 1712–5
[27] Tombler T W *et al* 2000 Reversible electromechanical characteristics of carbon nanotubes under local-probe manipulation *Nature* **405** 769–72
[28] Zhou X, Zhou J J and Ou-Yang Z C 2000 Strain energy and Young's modulus of single-wall carbon nanotubes calculated from electronic energy-band theory *Phys. Rev.* B **62** 13692–6
[29] Tu Z-c and Ou-Yang Z-c 2002 Single-walled and multiwalled carbon nanotubes viewed as elastic tubes with the effective Young's moduli dependent on layer number *Phys. Rev.* B **65** 233407
[30] Belytschko T *et al* 2002 Atomistic simulations of nanotube fracture *Phys. Rev.* B **65** 235430
[31] Xia Y Y *et al* 2002 Tensile strength of single-walled carbon nanotubes with defects under hydrostatic pressure *Phys. Rev.* B **65** 155415
[32] Wei C, Cho K and Srivastava D 2003 Tensile strength of carbon nanotubes under realistic temperature and strain rate *Phys. Rev.* B **67** 115407
[33] Dereli G and Ozdogan C 2003 Structural stability and energetics of single-walled carbon nanotubes under uniaxial strain *Phys. Rev.* B **67** 035416
[34] Wagner H D *et al* 1998 Stress-induced fragmentation of multiwall carbon nanotubes in a polymer matrix *Appl. Phys. Lett.* **72** 188
[35] Lourie O, Cox D M and Wagner H D 1998 Buckling and collapse of embedded carbon nanotubes *Phys. Rev. Lett.* **81** 1638
[36] Yu M F, Lourie O and Dyer M J 2000 Strength and breaking mechanism of multiwalled carbon nanotubes under tensile load *Science* **287** 637–40
[37] Demczyk B G *et al* 2002 Direct mechanical measurement of the tensile strength and elastic modulus of multiwalled carbon nanotubes *Mater. Sci. Eng.* A **334** 173–8
[38] Cuenot S *et al* 2003 Measurement of elastic modulus of nanotubes by resonant contact atomic force microscopy *J. Appl. Phys.* **93** 5650–5
[39] Salvetat J P *et al* 1999 Elastic and shear moduli of single-walled carbon nanotube ropes *Phys. Rev. Lett.* **82** 944–7
[40] Banhart F 1999 Irradiation effects in carbon nanostructures *Rep. Prog. Phys.* **62** 1181–221
[41] Iijima S, Ichihashi T and Ando Y 1992 Pentagons, heptagons and negative curvature in graphite microtubule growth *Nature* **356** 776
[42] Zhou O *et al* 1994 Defects in carbon nanostructures *Science* **263** 1744–7
[43] Charlier J C 2002 Defects in carbon nanotube *Acc. Chem. Res.* **35** 1063–9
[44] Saether E 2003 Transverse mechanical properties of carbon nanotube crystals. Part II: sensitivity to lattice distortions *Compos. Sci. Technol.* **63** 1551–9
[45] Ouyang M *et al* 2001 Atomically resolved single-walled carbon nanotube intramolecular junctions *Science* **291** 97
[46] Nardelli M B, Yakobson B I and Bernholc J 1998 Brittle and ductile behavior in carbon nanotubes *Phys. Rev. Lett.* **81** 4656
[47] Nardelli M B, Yakobson B I and Bernholc J 1998 Mechanism of strain release in carbon nanotube *Phys. Rev.* B **57** R4277
[48] Collins P G *et al* 2000 Extreme oxygen sensitivity of electronic properties of carbon nanotubes *Science* **287** 1001
[49] Ebbesen T W and Takada T 1995 Topological and SP3 defect structures in nanotubes *Carbon* **33** 973–8
[50] Liew K M, He X Q and Wong C H 2004 On the study of elastic and plastic properties of multi-walled carbon nanotubes under axial tension using molecular dynamics simulation *Acta Mater.* **52** 2521–7
[51] Duplock E J, Scheffler M and Lindan P J D 2004 Hallmark of perfect graphene *Phys. Rev. Lett.* **92** 225502
[52] Picozzi S *et al* 2004 Ozone adsorption on carbon nanotubes: the role of Stone–Wales defects *J. Chem. Phys.* **120** 7147–52
[53] Mielke S L *et al* 2004 The role of vacancy defects and holes in the fracture of carbon nanotubes *Chem. Phys. Lett.* **390** 413–20
[54] Yakobson B I 1998 Mechanical relaxation and 'intramolecularplasticity' in carbon nanotubes *Appl. Phys. Lett.* **72** 918
[55] Jiang H *et al* 2004 Defect nucleation in carbon nanotubes under tension and torsion: Stone–Wales transformation *Comput. Methods Appl. Mech. Eng.* **193** 3419–29
[56] Zhao Q, Nardelli M B and Bernholc J 2002 Ultimate strength of carbon nanotubes: a theoretical study *Phys. Rev.* B **65** 144105
[57] Samsonidze G G, Samsonidze G G and Yakobson B I 2002 Kinetic theory of symmetry-dependent strength in carbon nanotubes *Phys. Rev. Lett.* **88** 065501
[58] Zhou L G and Shi S Q 2003 Formation energy of Stone–Wales defects in carbon nanotubes *Appl. Phys. Lett.* **83** 1222
[59] Dumitrica T, Belytschko T and Yakobson B I 2003 Bond-breaking bifurcation states in carbon nanotube fracture *J. Chem. Phys.* **118** 9485–8
[60] Troya D, Mielke S L and Schatz G C 2003 Carbon nanotube fracture—differences between quantum mechanical mechanisms and those of empirical potentials *Chem. Phys. Lett.* **382** 133–41
[61] Belavin V V, Bulushev L G and Okotrub A V 2004 Modifications to the electronic structure of carbon nanotubes with symmetric and random vacancies *Int. J. Quantum Chem.* **96** 239–46

[62] Matern B 1960 *Spatial Variation* 2nd ed. (Berlin: Springer-Verlag)
[63] Lu Q 2005 Influence of randomly occurring defects on mechanical behavior of carbon nanotubes *PhD Thesis* Civil and Environmental Engineering Department, University of Delaware, Newark, DE
[64] Lu Q and Bhattacharya B 2005 The role of atomistic simulations in probing the small-scale aspects of fracture—a case study on a single-walled carbon nanotube *Eng. Fracture Mech.* at press
[65] Arroyo M and Belytschko T 2003 Nonlinear mechanical response and rippling of thick multiwalled carbon nanotubes *Phys. Rev. Lett.* **91** 215505
[66] Zhang P *et al* 2002 Fracture nucleation in single-wall carbon nanotubes under tension: a continuum analysis incorporating interatomic potentials *J. Appl. Mech.—Trans. ASME* **69** 454–8
[67] Zhang P *et al* 2002 The elastic modulus of single-wall carbon nanotubes: a continuum analysis incorporating interatomic potentials *Int. J. Solids Struct.* **39** 3893–906
[68] Zhang P *et al* 2004 An atomistic-based continuum theory for carbon nanotubes: analysis of fracture nucleation *J. Mech. Phys. Solids* **52** 977–98
[69] Li C and Guo W L 2003 Continuum mechanics simulation of post-buckling of single-walled nanotubes *Int. J. Nonlinear Sci. Numer. Simul.* **4** 387–93
[70] Li C Y and Chou T W 2004 Modeling of elastic buckling of carbon nanotubes by molecular structural mechanics approach *Mech. Mater.* **36** 1047–55
[71] Belytschko T *et al* 2002 Atomistic simulations of nanotube fracture *Phys. Rev.* B **65** 235430
[72] Huhtala M *et al* 2004 Improved mechanical load transfer between shells of multiwalled carbon nanotubes *Phys. Rev.* B **70** 045404
[73] Gumbsch P 1996 Brittle fracture processes modeled on the atomic scale *Z. Metallk.* **87** 341–8
[74] Machova A and Kroupa F 1997 Atomistic modelling of contribution of dislocations to crack opening displacements *Mater. Sci. Eng.* A **234–236** 185–8
[75] Marder M 1999 Molecular dynamics of cracks *Comput. Sci. Eng.* **1** 48–55
[76] Perez R and Gumbsch P 2000 Directional anisotropy in the cleavage fracture of silicon *Phys. Rev. Lett.* **84** 5347–50
[77] Swadener J G, Baskes M I and Nastasi M 2002 Molecular dynamics simulation of brittle fracture in silicon *Phys. Rev. Lett.* **89** 085503